

Plate deformation at depth under northern California: Slab gap or stretched slab?

Uri S. ten Brink

U.S. Geological Survey, Woods Hole, Massachusetts

Nobumichi Shimizu

Woods Hole Oceanographic Institution, Woods Hole, Massachusetts

Philipp C. Molzer

U.S. Geological Survey, Woods Hole, Massachusetts

Abstract. Plate kinematic interpretations for northern California predict a gap in the underlying subducted slab caused by the northward migration of the Pacific-North America-Juan de Fuca triple junction. However, large-scale decompression melting and asthenospheric upwelling to the base of the overlying plate within the postulated gap are not supported by geophysical and geochemical observations. We suggest a model for the interaction between the three plates which is compatible with the observations. In this "slab stretch" model the Juan de Fuca plate under coastal northern California deforms by stretching and thinning to fill the geometrical gap formed in the wake of the northward migrating Mendocino triple junction. The stretching is in response to boundary forces acting on the plate. The thinning results in an elevated geothermal gradient, which may be roughly equivalent to a 4 Ma oceanic lithosphere, still much cooler than that inferred by the slab gap model. We show that reequilibration of this geothermal gradient under 20-30 km thick overlying plate can explain the minor Neogene volcanic activity, its chemical composition, and the heat flow. In contrast to northern California, geochemical and geophysical consequences of a "true" slab gap can be observed in the California Inner Continental Borderland offshore Los Angeles, where local asthenospheric upwelling probably took place during the Miocene as a result of horizontal extension and rotation of the overlying plate. The elevated heat flow in central California can be explained by thermal reequilibration of the stalled Monterey microplate under the Coast Ranges, rather than by a slab gap or viscous shear heating in the mantle.

1. Introduction

Plate kinematic reconstructions commonly assume plate boundaries that have zero width throughout their thickness. This is reasonable for oceanic plate boundaries where the deformation zone is usually only a few kilometers wide. However, the deformation zone at a continental plate boundary can

be hundreds of kilometers wide. In California, reconstructions based on the above assumption predict asthenospheric upwelling into a gap in the underlying subducted slab ("slab gap") as a result of the northward migration of the unstable Pacific-North America-Juan de Fuca triple junction (Figure 1). As the triple junction migrates north, the subducting Juan de Fuca (JdF) plate slides out from beneath the North American plate, leaving a single-plate thickness where previously there was a double-plate thickness (Figure 1). Because the kinematic arguments in California are well established [Atwater, 1989], their consequences for geological interpretation have been accepted even when other interpretations of geological, geochemical, and geophysical data can be found. Here we suggest that perhaps a more realistic view of the plate boundary as a continuum with distributed deformation can reconcile the regional plate kinematics with the local geological, geochemical, and geophysical observations. We limit our model to the Coast Ranges, which are underlain by a relatively thin accretionary prism, because surface manifestation of asthenospheric upwelling should be readily recognizable in that region. We do not address a possible slab gap under the Great Valley or the Sierra Nevada, which are underlain by a thicker, more complex ophiolitic and Sierran arc crust and upper mantle [Godfrey *et al.*, 1997; Godfrey and Klemperer, 1998].

2. The Slab Gap Model

The geology of the west coast of North America during the last 150 Myr has largely been shaped by the subduction of the Farallon plate. Starting ~ 28-30 Myr ago, however, subduction brought the Pacific plate in contact with North America [Atwater, 1989](Figure 1a). Shortly thereafter, the Mendocino triple junction (MTJ) formed between the northern remnant of the Farallon plate (the Juan de Fuca plate), the North American (NOAM) plate, and the Pacific plate (Figure 1a). The triple junction has migrated northward relative to North America during the last ~20 Myr and subduction of the Juan de Fuca (JdF) plate was replaced by a right-lateral strike-slip (or transform) plate boundary (Figures 1 and 2). Upon cessation of subduction the weight of the already subducted plate continued to pull the slab downward, opening a gap into which sublithospheric material (asthenosphere) upwelled [Dickinson, 1997; Dickinson and Snyder, 1979a]. It is easy to visualize

Copyright 1999 by the American Geophysical Union.

Paper number 1999TC900050.
0278-7407/99/1999TC900050\$12.00

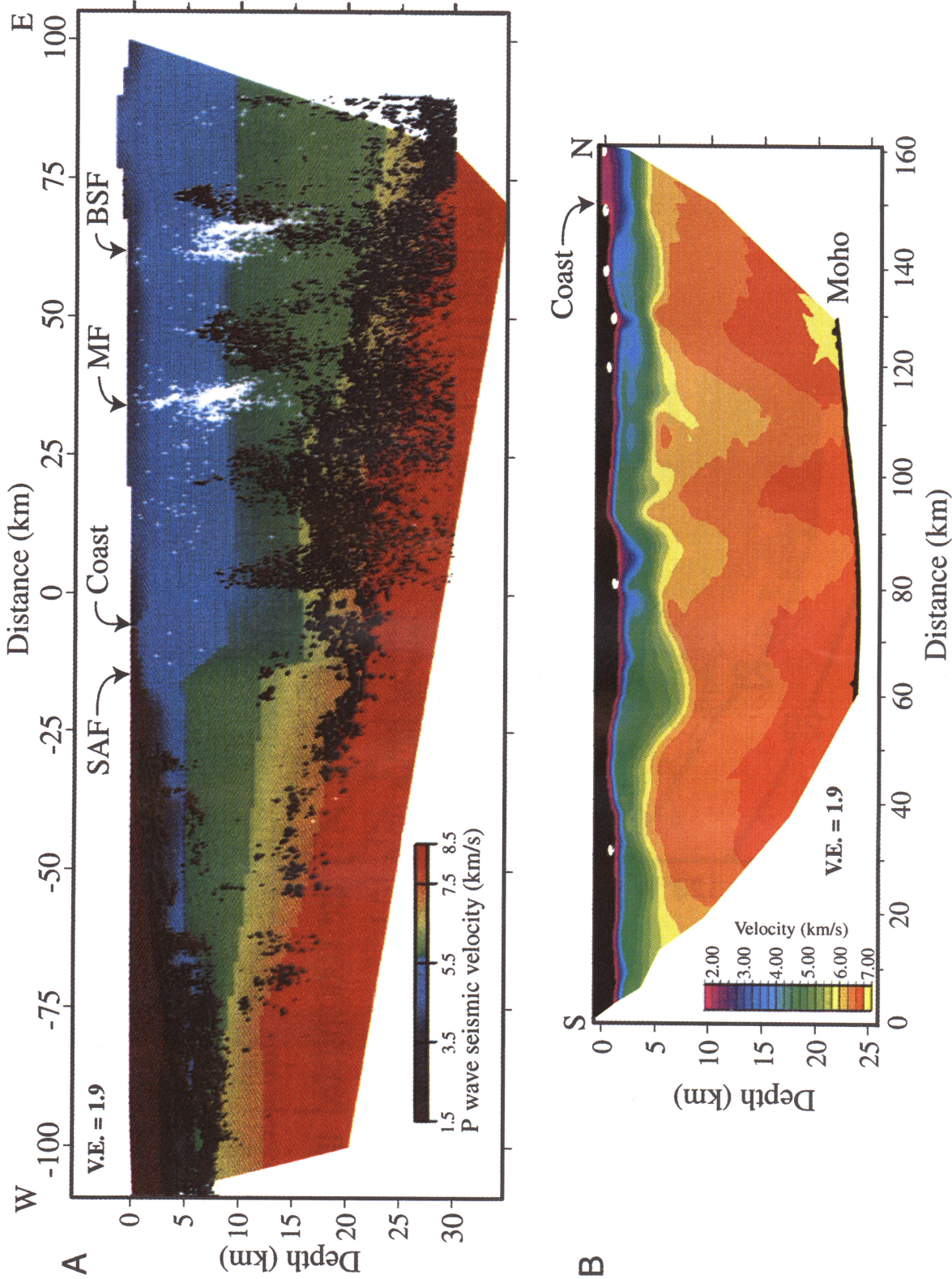


Plate 1. Comparison of crustal *P* wave velocity models from (a) northern California [Henstock et al., 1997] and (b) the Inner Continental Borderland [Ten Brink et al., 1999]. See Figure 2 for location. Black regions in Plate 1a are bright reflections and white dots are earthquake epicenters. SAF, San Andreas Fault; MF, Maacama Fault; BSF, Bartlett Fault. White dots in Plate 1b show the locations of recording stations. Air guns shots produced by the R/V Maurice Ewing at 50 m intervals along the line served as a seismic source. Note the different velocity color scale between Plates 1a and 1b.

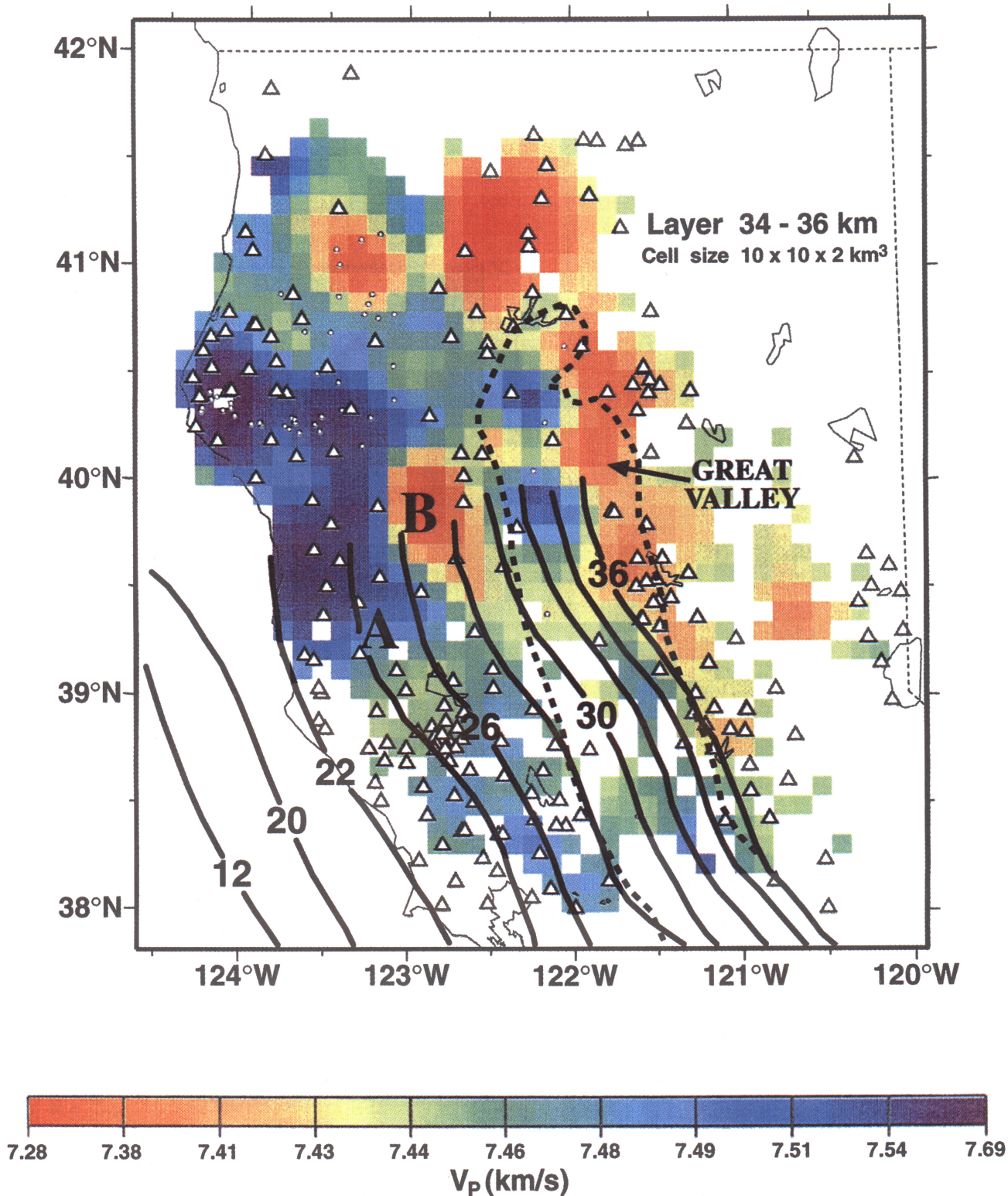


Plate 2. *P* wave velocity variations in a layer 34-36 km deep from travel time tomographic inversion of local earthquakes (H. Benz, written communication, 1998). Dashed line shows the location of the Great Valley. Contours of depth to Moho, based on the synthesis of seismic refraction profiles collected during the 1980s and 1990s between the Sierra Nevada and offshore California [Brocher *et al.*, 1999], show that west of the Great Valley this layer lies below the Moho. Note the lack of a regional low-velocity anomaly under the Coast Ranges, which would correspond to asthenospheric upwelling. Two local low-velocity anomalies were identified from this and other depth slices through the model, one anomaly (A) is between 22 and 30 km (therefore no anomaly is seen at the depth of this slice) and the other anomaly (B) is between 28 and 36 km. For details of the technique see the work of Benz *et al.* [1996]. Small circles show the epicentral locations. Triangles show the recording station locations.

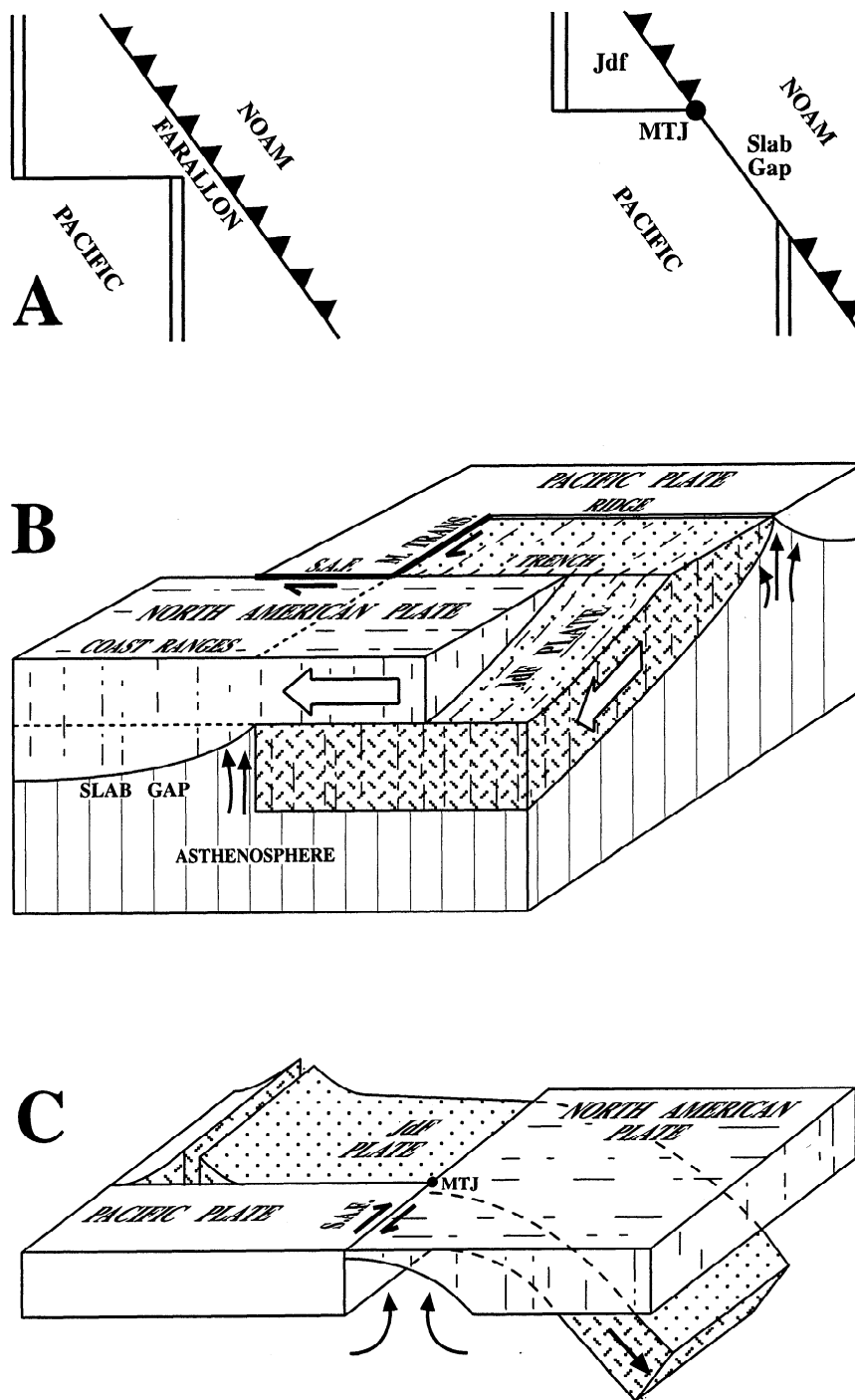


Figure 1. (a) Simplified plate motion prior to and after the collision of the Pacific-Farallon ridge with North America (NOAM). JdF, Juan de Fuca; MTJ, Mendocino triple junction. (b) Motion of Juan de Fuca and North American plates relative to a fixed Pacific plate near the Mendocino triple junction [after *Lachenbruch and Sass, 1980*]. A gap develops in the mantle lithosphere beneath NOAM as it slides off the JdF plate. SAF, San Andreas fault; M. trans - Mendocino fracture zone. (c) Side view of the slab gap assuming a vertical Pacific plate boundary along the San Andreas fault [after *Liu and Furlong, 1992*].

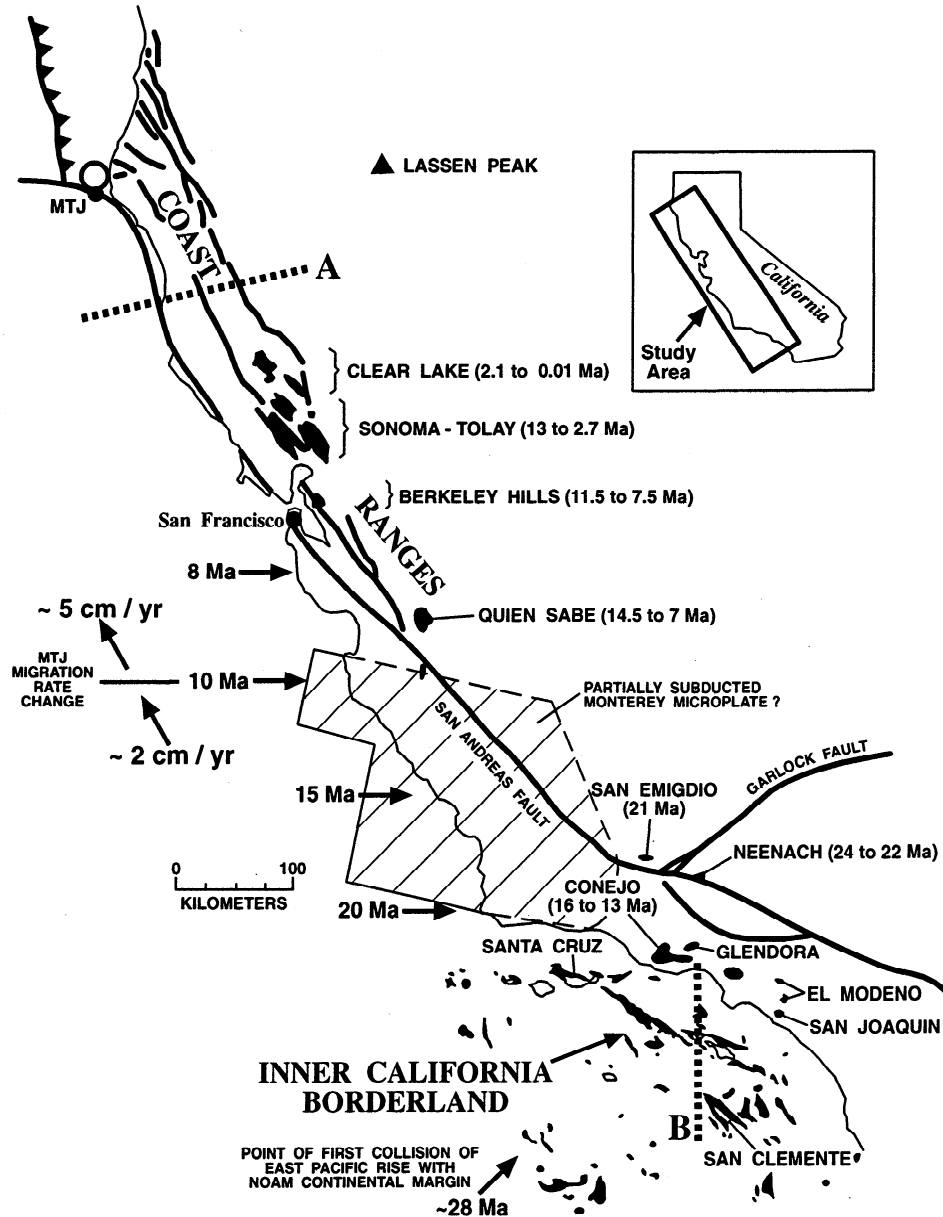


Figure 2. Generalized geologic map of coastal California showing the locations and ages of Neogene volcanic centers (solid regions [after *Johnson and O'Neil, 1984*]) and the position of the Mendocino triple junction (MTJ) at various times throughout the Neogene [*Atwater and Stock, 1998*]. The rate of this migration makes it possible to equate the distance from the present location of the MTJ at Cape Mendocino to any point farther south in California with the time since the MTJ swept through this point. Also shown are mid-Miocene volcanic outcrops in southern California [*Vedder, 1987*], which are related to the extension of the California Borderland, not to MTJ migration. Heavy dashed lines show the location of seismic velocity models in Plate 1. Heavy lines show the faults. Faults in northern California are after *Kelsey and Carver [1988]*. Open circle shows the location of the two strongest aftershocks of the 1992 Cape Mendocino earthquake [*Oppenheimer et al., 1993*].

the formation of the slab gap in a fixed Pacific plate reference frame, as a sideways (southward) slide of NOAM plate along the San Andreas fault (SAF) from an area underlain by subducted Farallon plate to an area where such a plate no longer existed (Figure 1b); [*Lachenbruch and Sass, 1980*]. Various predictions have been made based on the slab gap hypothesis.

The slab gap was envisioned to be the locus of decompression melting in the asthenosphere resulting in the accretion of a several kilometers thick layer of mafic material to the base of the California crust [*Liu and Furlong, 1992*]. Estimates of hydrocarbon maturation were made based on the thermal regime of a slab gap with asthenospheric upwelling [*Heasler and*

Surdam, 1985]. The Pacific-NOAM plate boundary was envisioned to be subhorizontal at depth (e.g., under the San Francisco Bay Area) and to migrate inland over time as the slab gap annealed [*Furlong et al.*, 1989; *Zandt and Furlong*, 1982].

3. Testing The Slab Gap Model

Several recent publications have questioned some aspects of the slab gap model [e.g., *Hole et al.*, 1998]. The geometry and timing of faults in the San Francisco Bay Area were shown not to fit the slab gap prediction of a subhorizontal plate boundary. Using rheological considerations, *Bohannon and Parsons* [1995] argued that a tear in the downgoing slab should occur at depths of ~100 km, which would place it considerably eastward of coastal California. Noting a continuous high basal velocity layer under the continental margin of central California, *Page and Brocher* [1993] suggested that Pacific plate lithosphere underlies the North American plate margin because a change in plate motions 3.5 Myr ago caused transpression between the two plates. *Henstock et al.* [1997] interpreted a continuous high-velocity basal layer that dipped eastward from the former trench out to 200 km farther east in northern California as a possible underplated JdF plate crust.

The size of the assumed gap may also be smaller than was previously assumed. Offshore magnetic anomalies and seismic evidence suggest that the central California margin and Coast Ranges may be underlain by the partially subducted Monterey microplate [*Miller et al.*, 1992, *Howie et al.*, 1993], which has been fully coupled to the Pacific plate since 18 Myr ago [*Nicholson et al.*, 1994](Figure 2). Therefore, only a ~430 km long section of the California Coast Ranges should be considered a candidate for a slab gap [*Atwater and Stock*, 1998]. This section, which extends from the MTJ to Monterey Bay, was swept by the migrating MTJ during the last 9 Myr.

The plate kinematic configuration itself may be more complicated than previously assumed. The slab-gap model is based on the configuration of three independently-moving rigid and competent plates, Pacific, NOAM, and JdF plates, but, in fact, the Pacific plate is the only rigid and competent plate. Nonrigid deformation of the JdF plate, known as the Gorda Deformation Zone, is manifested by curved magnetic anomalies and pervasive faulting [*Wilson*, 1986]. Deformation is pervasive despite the fact that the Gorda Deformation Zone is an oceanic plate whose top surface is at 0°C and has not yet even subducted under NOAM.

Neither does the NOAM plate in California behave as a single rigid plate. Several authors [e.g., *Walcott*, 1993; *Atwater and Stock*, 1998] have suggested that the Sierra Nevada/Great Valley block has been moving together with the Klamath Mountains (Figure 3). This block moved ~200 km northwestward relative to stable North America since 16 Ma and 130 km since 8 Ma, which represents ~30% of the total Pacific-NOAM motion during these time intervals [*Atwater and Stock*, 1998]. In a fixed Pacific plate reference frame the Klamath Mountains have then been moving southward faster than the California Coast Ranges have. The thickened NOAM crust in the Coast Ranges landward of the MTJ and south of the Klamath Mountains [*Beaudoin et al.*, 1998] may be the result of this relative motion. At any rate, NOAM is not a single block in the vicinity of the MTJ. It consists of two blocks, the

Sierra Nevada - Great Valley - Klamath Mountains block and the Coast Ranges. The latter is essentially a deformation zone between two more competent blocks, the Pacific plate and the Sierra Nevada - Great Valley block [*Walcott*, 1993] as geodetic measurements suggest [*Prescott and Yu*, 1986].

The slab gap model also assumes that the three plates are moving independently. This has not been the case for the JdF plate after the fragmentation of the Farallon plate. Starting 18 Myr ago, the JdF plate started rotating clockwise and seafloor spreading slowed [*Atwater*, 1989]. The clockwise rotation and the slowing of spreading aligned the JdF plate motion with respect to the Pacific closer to that of NOAM. This phenomenon has been most pronounced at the southern end of the plate, the Gorda Deformation Zone (Figure 3). The 1992 thrust earthquake beneath Cape Mendocino was followed by two M_s 6.6 aftershock within the JdF plate (see Figure 2 for location). The mechanism of these aftershocks indicates right-lateral, strike-slip motion on planes striking NW-SE at epicentral depths, which are within the JdF plate [*Oppenheimer et al.*, 1993]. Onshore, dextral strike-slip faults extend to the NNE across the MTJ, suggesting that some dextral motion of NOAM affects the area north of the MTJ [*Kelsey and Carver*, 1988](Figure 2).

4. Slab-Stretch Model

We propose an alternative model based on kinematics of non rigid plate boundaries with a lithospheric thermal history, which explains the geochemical and geophysical observations. In this model, continuous deformation, rotation, and stretching of the JdF plate fill the geometrical gap without large-scale holes and tears (Figures 3 and 4).

The large and rigid Pacific plate is moving northwestward in a hot spot frame of reference [*Atwater and Stock*, 1998](Figure 3) pushing at the Juan de Fuca plate across the Mendocino Fracture Zone and causing it to move northward. Although the fracture zone may be weak in shear, north-south oriented normal compressive stresses can be transmitted to the southern part of the plate [*Wang et al.*, 1997]. Landward of the MTJ, however, the subducting Juan de Fuca plate is not pushed by the Pacific plate and, in fact, is not confined. This allows the plate to spread into the unconfined region. The spreading may be analogous to the "westward spreading" of western North America, i.e., the extensional and rotational deformation, attributed by some to the northwestward retreat of the Pacific plate away from North America [*Walcott*, 1993; *Atwater and Stock*, 1998].

A more quantitative analysis for the forces acting on the Juan de Fuca plate [*Wang et al.*, 1997] further illuminates how the slab stretch may occur. The main forces acting on the Juan de Fuca plate are the northward transform push across the Mendocino Fracture Zone and the strike-parallel subduction resistance force which balances it [*Wang et al.*, 1997](Figure 5a). Subduction resistance is the viscous drag on both the upper surface and the lower surface of the slab. The absolute motion of the Juan de Fuca plate and its motion relative to North America are roughly parallel to each other (northeastward) and can thus be treated as the combined resistance. The subduction resistance force can be separated into directions orthogonal and parallel to the subduction zone. The orthogonal compo-

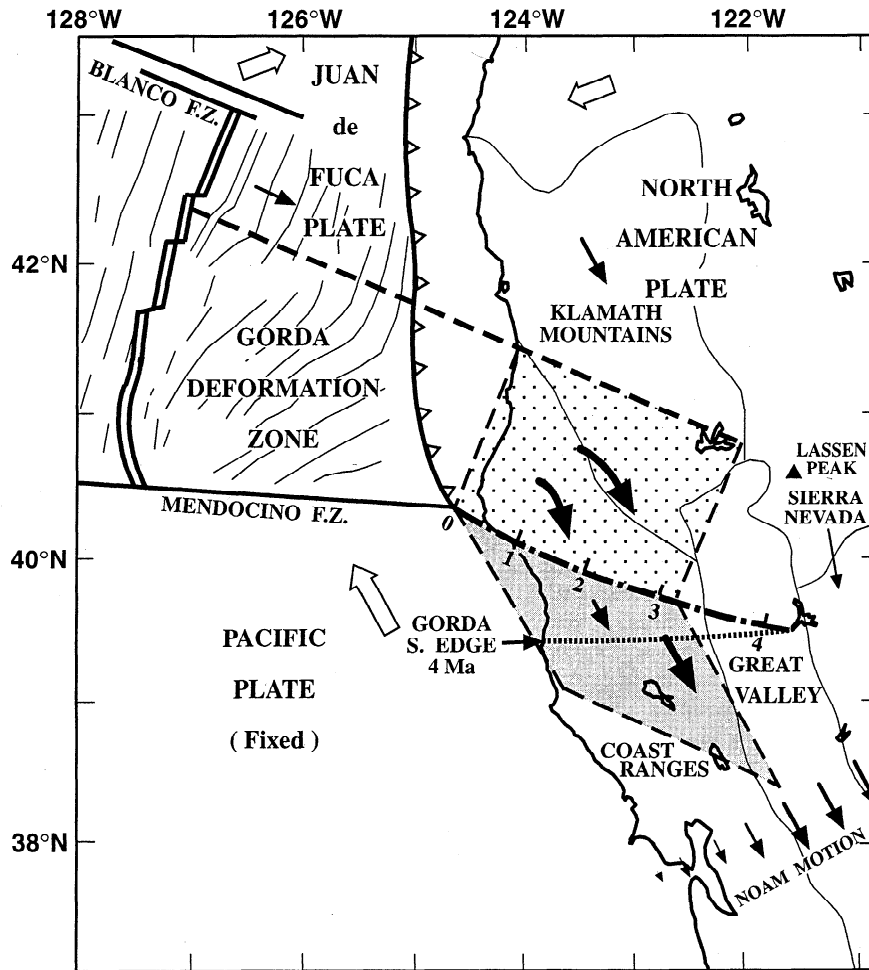


Figure 3. Simplified map of the Mendocino triple junction area and the extent of the subducted Juan de Fuca (JdF) plate. Dotted area is the estimated subducted JdF area during the last 3.2 Myr, determined by the southern edge of the subducted plate (dash-dotted line with numbers corresponding to age in megayears) [Wilson, 1986] and the trajectory of the northern edge of the Gorda Deformation Zone (GDZ) parallel to the Blanco Fracture Zone (heavy dashed line). This trajectory extends to the northern edge of the Great Valley and is also the northern limit of strike-slip faults in northern California (Figure 2). Shaded area is the estimated slab gap area under the Coast Ranges assuming a constant North American plate relative motion of 5 cm yr^{-1} during the past 3.2 Myr. However, the actual gap area to be filled by the stretching of the JdF slab is only approximately one-half of the shaded area, because North America motion tapers off from the Great Valley toward the San Andreas fault [Prescott and Yu, 1986]. Another estimate for the gap area during the last 4 Myr is given by the area bounded by the southern edge of the Gorda Deformation Zone at 4 Ma [from Atwater and Stock, 1998] and the estimated present southern edge of the JdF plate (dashed-dotted line) [Wilson, 1986]. Heavy arrows represent rotation and stretching of the subducted JdF slab to fill the geometrical gap. Small arrows represent plate motion in a fixed Pacific reference. Open arrows represent Pacific, North American, and JdF plate motion in an "absolute" (hot spot) frame of reference [Wang et al., 1997].

ment (east-west in the southern JdF plate) balances the slab pull force, which is orthogonal to and directly downdip of the subduction zone [Wang et al., 1997]. The parallel component is oriented south and balances the transform push force seaward of the MTJ. However, there is no force to balance the strike-parallel force landward of the MTJ; hence rotation and stretching can occur in this area as shown by the finite element model of Wang et al. [1997] (Figure 5b).

We propose that the geometrical gap predicted by a rigid plate model is filled by continuous deformation without large

holes and tears due to rotation and stretching of the JdF plate (Figures 3 and 4). The size of the gap can be estimated from the length of the area predicted by rigid plate kinematics to have opened during the last 3.2 Myr (shaded area in Figure 3), calculated assuming an average migration rate of 5 cm yr^{-1} . However, NOAM motion relative to the Pacific plate decreases from the Great Valley to zero offshore [Prescott and Yu, 1986], implying that the Coast Ranges are increasingly dragged by the Pacific plate. For simplicity, therefore, we consider that only one-half of the shaded area (Figure 3) constitutes the gap. One-

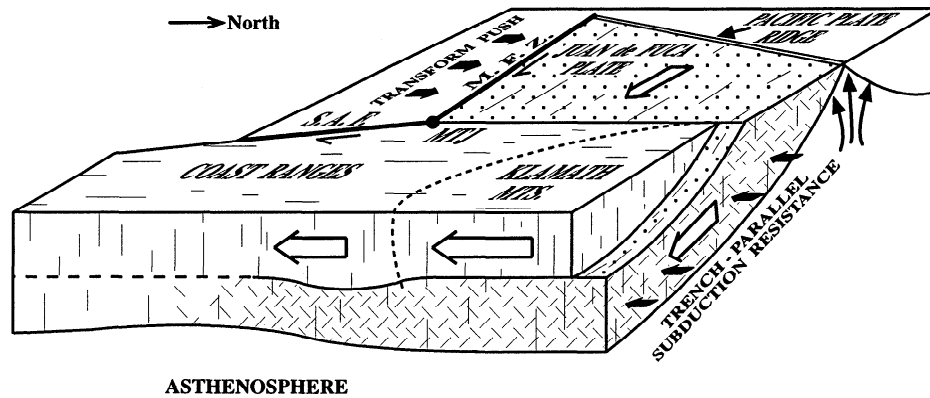


Figure 4. Alternative cartoon to Figure 1b showing continuous plate deformation filling the geometrical slab gap (slab stretch model), the forces acting on the southern end of the Juan de Fuca plate, and the transient thickening of the overlying North American plate due to faster motion of the Klamath Mountains -Sierra Nevada block relative to the Coast Ranges. See text for details.

half of the shaded area is only 37% of the JdF plate area subducted during this time [Wilson, 1986](Figure 3). If the JdF slab stretches to fill this gap, it will have to thin by a factor of only 1.37. An alternative estimate of the predicted gap from rigid plate kinematics is the difference between the placements of the southern edge of the JdF plate 4 Myr ago and at present [Atwater and Stock, 1998](Figure 3). The triangular area between these two placements is only 27% of the JdF plate area subducted during the past 4 Myr [Wilson, 1986](Figure 3).

The age of the subducted plate is 6-10 Ma [Wilson, 1986]; hence the thickness of the thermal lithosphere (to a temperature of 1300°C) is 25-30 km. Thinning by a factor of 1.37 reduces the slab's thermal thickness to 18.1-21.7 km, which is equivalent to the thickness of a 4 Ma slab. (Thinning of the

subducted slab by a factor of 1.27 reduces the thermal thickness of the lithosphere to 19.7-23.6 km, which is equivalent to the thickness of a 4-5 Ma slab.) Thinning of the mantle at these shallow depths (40-50 km) and by this factor is expected to generate only negligible decompression melting of the upper mantle [McKenzie and Bickle, 1988]. Strain may not be uniform, so larger amounts of thinning may take place locally as the tomographic images, discussed in section 6, may suggest.

The depth and expected temperature range (Figure 6) for the JdF plate underlying the Coast Ranges indicate that its rheology under tension at the strain rates corresponding to the above factors of stretching ($2-3 \times 10^{-15} \text{ s}^{-1}$) may be in the brittle-ductile transition regime [Brace and Kohlstedt, 1980]. It is possible, especially under the thinner western part of the

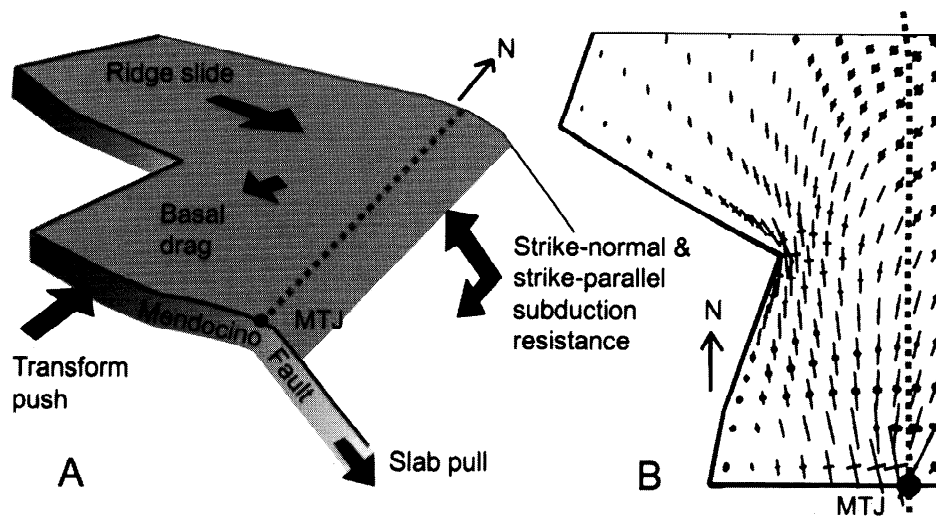


Figure 5. (a) Forces acting on the southern part of the Juan de Fuca (JdF) plate [from Wang *et al.*, 1997]. (b) Stress field in the southern JdF plate calculated by a plane stress finite element method for an elastic lithospheric plate (modified from Model V2 of Wang *et al.* [1997]). This model includes a 50 km wide zone of the subducted slab landward of the trench (dashed line). Thin bars show the compressive stresses. Thick bars show the tensile stresses. Note the rotation and stretching landward of the Mendocino triple junction, because transform push is absent there.

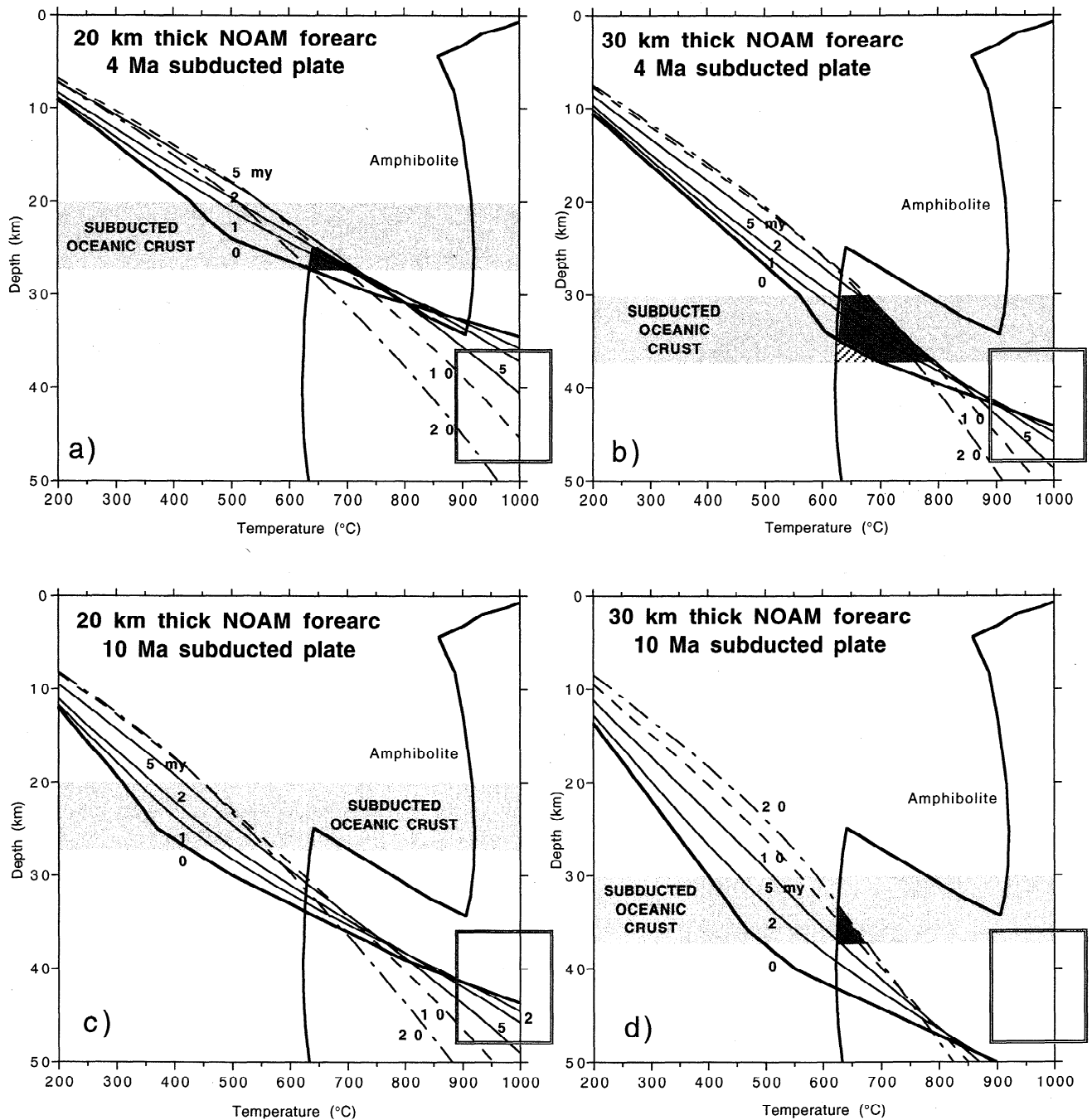


Figure 6. (a-d) Calculated geothermal gradients as a function of time after cessation of subduction (time 0) for subducted slabs with a thermal age of 4 and 10 Ma overlain by 20 and 30 km thick North American plate. (e) Simplified geothermal gradients as a function of time for a partial slab gap (no mantle lithosphere), shown for comparison with Figures 6a - 6d. In the initial geothermal gradient, which is equivalent to a 0.6 Myr old subducted slab, a temperature of 1300°C is placed at the base of the subducted slab 7 km beneath a 20 km thick North American plate. Also shown are solidi for amphibolite (solid line in Figures 6a - 6e) [Wyllie and Wolf, 1993] and for red clay, dry basalt, and peridotite solidi (solid lines in Figure 6e; [Nichols *et al.*, 1996; Peacock, 1996]). Partial melt of the oceanic crust is expected only at depths where temperatures are higher than the amphibolite solidus (dotted regions), but more voluminous melting at the base of the former forearc, the subducted oceanic crust, and the subducted mantle lithosphere is expected in a slab gap model (Figure 6e). Some melting may occur even before cessation of subduction (cross-hatched regions). Boxes show the thermobarometric estimate based on spinel lherzolites in xenoliths of Pliocene (2.5-3.6 Ma) basalt along the Calaveras fault north of Quien Sabe [Jove and Coleman, 1998]. Calculated geothermal gradients for a 4 Ma slab (Figure 6a) 5-10 Myr after cessation of subduction and stretching fall within this temperature-depth estimate, but those for a slab gap (Figure 6e) predict much higher temperatures at this depth range.

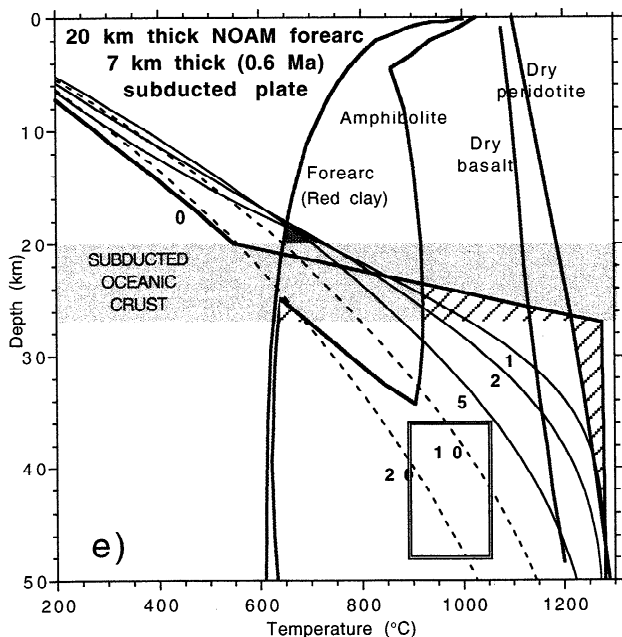


Figure 6. (continued)

Coast Ranges, that temperatures in the underplated JdF oceanic crust are low enough to allow brittle deformation. The vertical offsets in the subducted slab of northern California [Henstock *et al.*, 1997; Plate 1a) may be manifestations of this brittle regime. Under the eastern part of the Coast Ranges and at a deeper level of the JdF lithosphere, ductile deformation probably takes place [Molnar, 1992]. Strain rate is governed by temperature; hence the lower part of the slab is expected to thin faster than the upper part of the slab. On the other hand, the oceanic crust is more felsic than the mantle lithosphere and therefore it may deform faster [Brace and Kohlstedt, 1980]. Uncertainties in the activation energy for olivine and diabase yield an uncertainty in creep strength of at least a factor 10 at the temperature range of the subducted oceanic crust (Figure 6), making more accurate analysis futile [Molnar, 1992].

5. Thermal and Magmatic Consequences of the Slab Stretch Model

With the slab stretch model in mind, we envision the thermal evolution of the lithosphere to be the result of thermal reequilibration following cessation of subduction and some stretching of the slab. The overlying plate is the forearc region of the subduction zone. This region cools during subduction [e.g., van der Beukel and Wortel, 1988], because the cold surface of the subducting plate is underthrust beneath the forearc. This cooling effect is generally manifested by the low surface heat flow in forearc regions ($<45 \text{ mW m}^{-2}$). The geothermal gradient in the forearc depends on the rate of subduction and the age of the subducting plate [Dumitru, 1991]. When subduction and stretching stop, thermal reequilibration begins, and the temperature at the base of the forearc rises.

We approximate this process by calculating the geothermal gradients as a function of time after cessation of subduction

(time 0) for subducted slabs with a thermal age of 10 and 4 Ma overlain by 20 and 30 km thick forearc. Initial temperature gradients in our calculations are Dumitru's [1991] thermal gradients for 10 and 4 Ma subducted lithosphere and overlying North American plate thicknesses of 20 and 30 km. His calculations use a two-dimensional finite difference grid assuming steady state ($\sim 50 \text{ Myr}$) subduction, a subduction rate of $\sim 40 \text{ km my}^{-1}$, a subducting slab $\leq 10 \text{ Ma}$, and a subduction angle of $\sim 15^\circ$ [Dumitru, 1991, and references therein]. Our finite-difference numerical calculations used a vertical grid of 1 km to a depth of 125 km, time step of 8000 years, bottom and surface temperatures of 1300°C and 0°C , respectively, specific heat of $1 \text{ J kg}^{-1} \text{ }^\circ\text{C}^{-1}$, forearc and slab thermal conductivities of 2.5 and $3.3 \text{ W m}^{-1} \text{ }^\circ\text{C}^{-1}$, and an exponential radiogenic heat production within the overlying forearc with a "skin depth" of 10 km and a surface production rate of $1.2 \mu\text{W m}^{-3}$. Horizontal conduction across the former forearc was neglected following James *et al.* [1989]. Lateral conduction due to localized areas of high strain was ignored for the sake of simplicity and clarity. Initial heat flow is higher than that calculated (Figure 7), because the forearc region was cooler at the end of subduction than that determined from the steady-state calculations (i.e., assuming a constant age of subducting plate) [Dumitru, 1991]. Much older slab entered the trench during much of the time prior to cessation and stretching. However, the amount of later transient heating during initial reequilibration is also larger, and the overall effect on the results is small.

There are two important consequences of thermal reequilibration: (1) melting of the subducted crust and (2) elevated heat flow in the overlying plate. Minor volcanic activity occurred in the wake of the northward passage of the MTJ, reflected in the northward younging of volcanic outcrops (Figure 2) [Dickinson, 1997; Dickinson and Snyder, 1979a]. Present-day activity ($< 2 \text{ Ma}$) is located at Clear Lake. It has been suggested that the volcanism resulted from a slab gap under the forearc [Dickinson and Snyder, 1979b; Johnson and O'Neil, 1984]. Quantitative estimates of asthenospheric upwelling into the gap, however, predict voluminous magmatic production [Liu and Furlong, 1992], far more voluminous than the geologic data suggest. In the slab stretch model we explain the volcanism as mainly arising from crustal anatexis. Figure 6 illustrates the magnitude of temperature rise at the subducted oceanic crust and base of the overlying forearc as a function of thermal age of the subducted slab and of forearc thickness. Pressure-temperature conditions of the amphibolite solidus (temperatures $\geq 630^\circ\text{C}$ at depths $\geq 25 \text{ km}$) [Wyllie and Wolf, 1993] can be attained during the first 5 Myr after the cessation of subduction of a young ($\sim 4 \text{ Ma}$) oceanic crust overlain by 20-30 km thick crust (dotted region in Figure 6). In fact, subduction of very young oceanic slab can lead to slab melting even before subduction ceases (cross-hatched regions in Figures 6b and e) [Defant and Drummond, 1990; Peacock, 1996]. For older subducted oceanic crust (e.g., 10 Ma, Figures 6c and 6d) or thinner overlying forearc, these conditions are either not met or are met more than 5 Myr after subduction has ceased (Figure 6d). Dehydration melting of amphibolite would cease immediately after small volumes of melt are produced, because water released by dehydration is immediately dissolved into melt, thereby "drying-up" the system; in other words, the vapor present solidus (Figure 6) no longer applies. Magma-

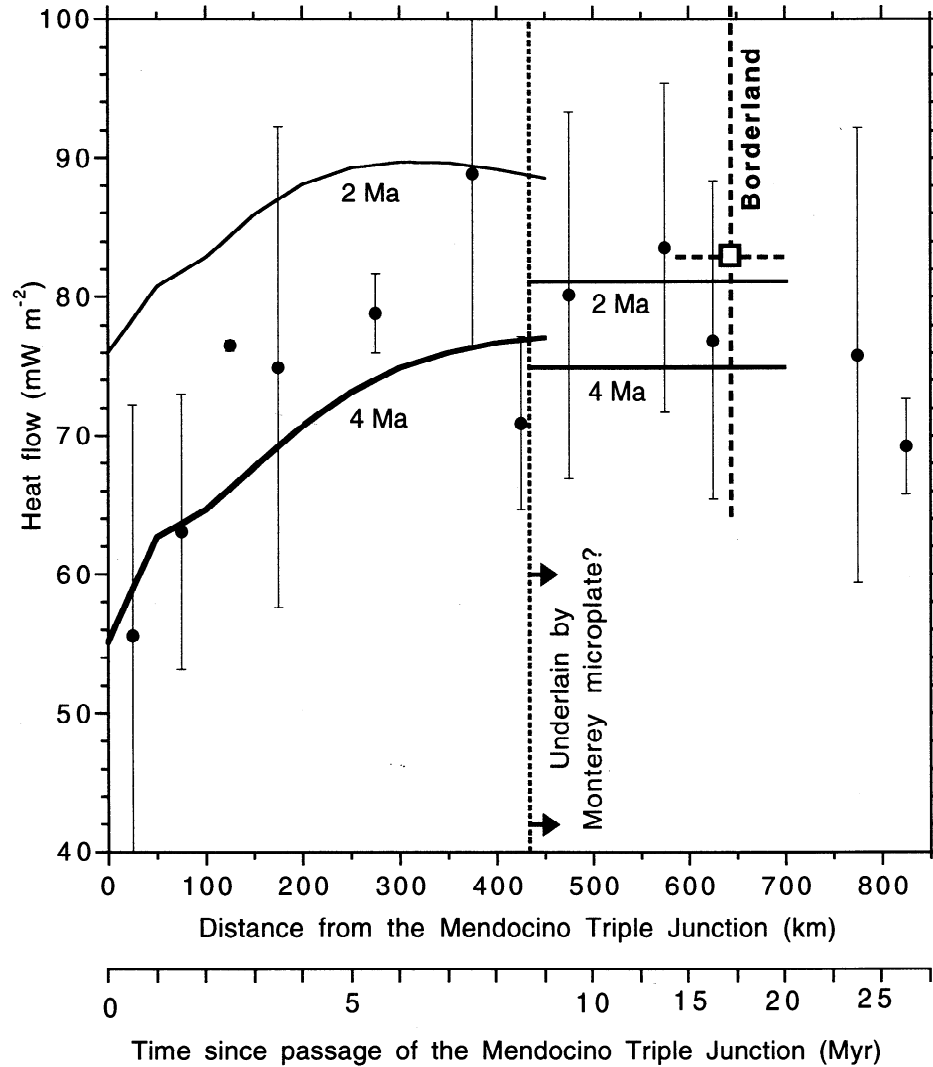


Figure 7. Surface heat flow in western California as a function of distance from the Mendocino triple junction (MTJ) and time since the MTJ passed through the measurement location [Lachenbruch and Sass, 1980; Sass *et al.*, 1997]. Heat flow was averaged over 50 km bins with error bars showing one standard deviation. Also marked for comparison is the mean heat flow for the California Inner Continental Borderland [Lee and Henyey, 1975] with a range showing one standard deviation (dashed line). It is plotted at an age range of 14–20 Myr, the age range for extension and volcanism in the Inner California Borderland. Curves represent calculated heat flow values from geothermal gradients in Figure 6 for a forearc thickness of 20 km and thermal age of subducted slab of 4 and 2 Ma. The data are best fit by a curve representing a setting with an overlying forearc thickness of 20 km and a subducting slab thermal age of 4 Ma or slightly younger without a slab gap. Heat flow beyond 430 km from the MTJ (vertical gray dashed line) may simply be due to reequilibration of the geothermal gradient after the young Monterey microplate stalled under central California 18 Myr ago [Nicholson *et al.*, 1994; Atwater and Stock, 1998]. Horizontal lines represent the calculated heat flow 18 Myr after cessation of 2 and 4 Myr old subducted lithosphere. Lines are horizontal because simultaneous cessation of subduction is assumed along the microplate's boundary with North America. Note that neither a slab gap nor shear heating of the upper mantle is needed to explain the heat flow in central California.

tism in California is typically short lived and produces small volumes of magma. It occurs mainly in the eastern part of the Coast Ranges [Johnson and O'Neil, 1984] where the overlying crustal thickness reaches 20–25 km [Henstock *et al.*, 1997]. A seismic profile across northern California where the MTJ was located < 2 Myr ago shows "bright spots" which cluster throughout the fossil oceanic crust (Plate 1a). These

have been interpreted to represent melt lenses [Levander *et al.*, 1998]. These observations are consistent with the suggestion that the mid-Cenozoic and younger volcanism that occurs in the wake of the northward migration of the MTJ results dominantly from anatexis of oceanic crust and not from decompression melting of the asthenosphere.

The composition of volcanic rocks along the California

Coast Ranges also supports our model. The volcanic rocks are dominantly intermediate to silicic, have relatively high $^{87}\text{Sr}/^{86}\text{Sr}$ ratios (0.704-0.706; few samples with ratios of 0.7025-0.704 have Th-Ta-Hf ratios similar to the other rocks), relatively high $\delta^{18}\text{O}$ values (7.5-11.5), and relatively high Th contents, suggesting that crustal anatexis played a dominant role in their generation. It was proposed that slab gap induced asthenospheric upwelling triggered melting of the overlying forearc [Johnson and O'Neil, 1984], but it does not explain why only small volumes of short-lived volcanism are produced and why asthenospheric-derived melts are rare. Trace element abundance of the Clear Lake Volcanics [Hearn et al., 1981], the youngest surface manifestation of the process, are characterized by strong light rare earth element (REE) enrichment and are consistent with crustal anatexis origin. In contrast, asthenospheric-derived melts (e.g., mid-ocean ridge basalts) are predominantly light REE depleted [Hofmann, 1988].

Surface heat flow in western California increases rapidly immediately south of the MTJ, reaching maximum several hundreds of kilometers to the south and then decreasing slightly. Our calculations best fit the data with an overlying crustal thickness of 20 km and an underlying stretched oceanic slab with an equivalent thermal age of 4-2 Ma (Figure 7). The pattern of increasing heat flow south of the MTJ was previously cited as evidence for a slab gap [Lachenbruch and Sass, 1980]. Interestingly, however, these authors pointed out that the heat flow variations are best fit with cooler than asthenospheric temperatures (1000°C) emplaced instantaneously at the base of a 20-km-thick crust.

Heat flow beyond a distance of 430 km from the MTJ is neither due to a slab gap nor due to a slab stretch (Figure 7). It may simply be the result of reequilibration of the forearc temperatures following the cessation of subduction when the Monterey microplate stalled and was captured by the Pacific plate (Figure 2) ~18 Myr ago [Nicholson et al., 1994; Atwater and Stock, 1998]. This point is further elaborated on in section 8.

Our proposed geothermal gradient (Figure 6a) also matches thermobarometric estimates from spinel ilmenite [Jove and Coleman, 1998] from Coyote Reservoir (east of the San Francisco Bay area and 30 km north of Quien Sabe, Figure 2). These upper mantle xenoliths erupted with small quantities of alkali-olivine basalt along the Calaveras fault during the Pliocene (2.5-3.6 Ma), possibly due to fault-stepping interaction [Jove and Coleman, 1998]. The overlying forearc thickness in this region is 20 km [Brocher et al., 1999]. The MTJ passed by this latitude 8 Myr ago, although Coyote Reservoir itself may have been originally farther south and migrated later by strike-slip deformation [e.g., Johnson and O'Neil, 1984]. We therefore estimate that these xenoliths erupted 5-10 Myr after the MTJ passed by this outcrop. Our proposed geothermal gradients 5 and 10 Myr after the cessation of subduction and stretching are centered on the estimated range of temperatures and depths from these samples (box in Figure 6a). The fit is less satisfactory for a 20 km thick forearc and a 10 Ma thermal age or for a 30 km thick forearc and a 4 Ma thermal age. The fit to the estimated temperatures and depths is poor for calculated geothermal gradients 5 and 10 Myr after the introduction of asthenospheric temperatures in a slab gap model (Figure 6c).

6. Other Observations

In this section we review different geophysical and geological observations which we believe are consistent with a slab stretch model and the thermal structure that it predicts. Seismic refraction data [Brocher et al., 1999, and references therein] beneath the Coast Ranges show a high-velocity basal layer which is compatible with a fossil subducted oceanic crust. Particularly noteworthy is the existence of a continuous high-velocity basal layer (yellow colors in Plate 1a) that dips eastward from the trench out to 200 km farther east in an area where the MTJ passed only < 2 Myr ago (Plate 1a). This observation directly contradicts the slab gap hypothesis, although a suggestion was made that decompression melting of asthenospheric mantle within the gap was followed by underplating of a 4-5 km thick layer of basalt to the base of the crust [Liu and Furlong, 1992]. The P wave velocity directly below the Moho in northern California, however, is $\geq 8 \text{ km s}^{-1}$ [Henstock et al., 1997], a value too high for a partially molten upper mantle. Additionally, the surface heat flow resulting from underplating a 4-5 km thick layer of basalt is expected to be much higher than that observed unless the top of the layer resides deeper than 30 km depth [Liu and Furlong, 1992]. Seismic refraction data in northern California, however, indicate that the layer is substantially shallower than 30 km throughout the Coast Ranges [Beaudoin et al., 1996; Brocher et al., 1999; Godfrey et al., 1997; Henstock et al., 1997] (Plate 1).

A regional low-velocity zone in tomographic images of the upper mantle beneath northern California was previously cited in support of the existence of asthenospheric upwelling on a regional scale [Benz et al., 1992; Zandt and Furlong, 1982]. The tomographic studies on which the images were based ignored crustal velocity and crustal thickness variations which contribute to the travel time delay (H. Benz, personal communication, 1998). Recent tomographic images of the crust and shallow mantle beneath northern California using local earthquake sources and the permanent northern California seismic stations (H. Benz, written communication, 1998) show no evidence for a regional low-velocity zone within the shallow upper mantle (e.g., Plate 2). Only two local (50x50 km) pockets of low-velocity material in the upper mantle are observed in the tomographic images (anomalies marked A and B in Plate 2) which may indicate localized zones of higher strain.

7. Continental Borderland - A Slab Gap in Coastal California?

The purpose of this section is to illustrate the expected thermal and magmatic consequences from a slab gap under a forearc region of the former subduction zone. We discuss observations from the Inner Continental borderland (ICB) offshore southern California where a local slab gap may have formed [ten Brink et al., 1999]. We compare these observations with similar ones in northern California, where the slab gap model was promoted. The probable slab gap in the ICB was formed by extension, uplift, and translation of the margin 20-18 Ma [Nicholson et al., 1994] (Figure 8).

The volume and composition of volcanic rocks in southern California differ from those in central and northern California (Figure 2). There are thick sections (>500 m) of 18-14 Myr old volcanic rocks [Crouch and Suppe, 1993; Cole and Basu,

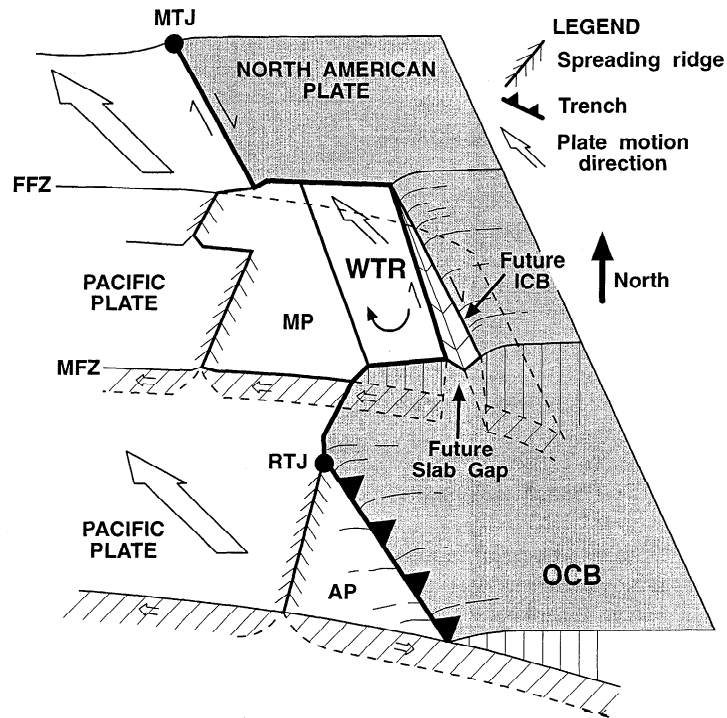


Figure 8. Model for the development of the Inner Continental Borderland (ICB) 20-18 Myr ago in the wake of the rotation and translation of the Western Transverse Ranges (WTR) (after *Nicholson et al.*, 1994). The rotation and translation of the WTR followed the capture of the subducted Monterey microplate (MP) by the Pacific plate and resulted in a high extension rate and a gap in the fossil subducted Farallon plate. OCB, Outer Continental Borderland; FFZ, Farallon Fracture Zone; MFZ, Morro Fracture Zone; RTJ, Rivera Triple Junction; AP, Arguello Microplate.

1995; *Dickinson*, 1997], often with mafic to intermediate composition. Petrogenesis of these volcanic rocks and trace element composition indicate that they were derived by an interaction of a very young, depleted oceanic lithosphere with the continental margin [*Cole and Basu*, 1995]. The rocks have $^{87}\text{Sr}/^{188}\text{Sr}$ ratios (0.7025-0.7038) and $\delta^{18}\text{O}$ values (5-7.5) close to mid-ocean ridge basalt (MORB) ratios, suggesting that they were derived mainly from a mantle source [*Johnson and O'Neil*, 1984]. With asthenospheric temperatures at the base of the fossil subducted oceanic crust, melting of amphibolite is expected during and for the first few million years following extension, when basal crustal temperatures at the base of the crust are above 920°C (Figure 6e). Some melting of the base of the overlying crust is also expected, and temperatures in much of the middle and lower crust allow for ductile flow. Finally, adiabatically rising asthenospheric mantle with a normal potential temperature will undergo decompression melting when it ascends to depths less than 60 km [*McKenzie and Bickle*, 1988].

Heat flow in southern California is unusually high, particularly in the ICB where values reach between $83 \pm 18 \text{ mW m}^{-2}$ (Figure 7) [*Lee and Henyey*, 1975]. These values are generally higher than would be expected from cooling and reequilibration of a 4 Ma slab which stopped subducting 20-28 Myr ago (Figure 7). However, if we assume that extension brought asthenospheric temperatures to 27 km depth some 18-20 Myr

ago (Figure 6e), then the calculated present heat flow ($83\text{-}86 \text{ mW m}^{-2}$) falls within the observed range [*ten Brink et al.*, 1999]. The Pacific-NOAM plate boundary was centered on the ICB until 12 Ma, and some tectonic activity probably continued in the ICB until 5 Ma [*Nicholson et al.*, 1994]. Even with a possible contribution to the increased heat flow from this later activity, the ICB heat flow is still higher than the heat flow from most of the Coast Ranges. Although the crust of the ICB was replaced by Catalina Schist 20-18 Myr ago with additional magmatic input lasting until 14 Myr ago [*ten Brink et al.*, 1999], the advective heat from these processes has long dissipated. Advective heat was ignored in the calculations of Figure 6e.

Unlike northern California (Plate 1a), seismic P wave velocity models of the ICB do not show high basal velocities associated with a fossil subducted oceanic crust (Plate 1b). The velocity models show relatively low velocities to the Moho, interpreted as Catalina Schist [*ten Brink et al.*, 1999]. The seismic refraction data consist only of upper crustal refractions (P_g) and Moho wide-angle reflections (P_mP). Upper mantle refractions (P_n) with an apparent velocity of $7.7\text{-}7.9 \text{ km s}^{-1}$ were observed only on a single unreversed seismic record [*ten Brink et al.*, 1999].

In summary, high heat flow, voluminous volcanism, a rather primitive isotopic composition of the magmas, and the absence of a high P wave velocity basal layer are observed in the Inner

Continental Borderland (ICB) offshore southern California. We would expect similar observations in northern California, if a regional slab gap existed there.

8. Discussion: Is There a Stress-Heat Flow Paradox in California?

Although the difference between the slab stretch and slab gap models can be perceived as simply a difference in the degree of reheating the North American plate, we believe that the implications to the understanding of upper mantle deformation are significant. We have already discussed the fact that a slab stretch model implies spreading of the mantle lithosphere to fill gaps. Here we discuss another implication of our model: the so-called "stress-heat flow paradox" [e.g., Molnar, 1992]. There is no measurable increase of heat flow near the San Andreas fault in central California, but there is a broad zone of high heat flow across the entire Coast Ranges averaging 30 mW m^{-2} higher than that typical for continental regions. We focus our discussion on the regional heat flow. The regional high heat flow was explained as a result of shear heating on horizontal planes due to viscous drag of the upper part of the lithosphere over its substratum [Lachenbruch and Sass, 1973], shear heating on vertical planes in the lithospheric upper mantle along the Pacific-North American diffuse plate boundary [Molnar, 1992], and the effect of the slab gap [Lachenbruch and Sass, 1980]. The shear heating argument was used to estimate the magnitude of shear stresses in the mantle lithosphere and to argue about the necessary rheology to support them [Molnar, 1992].

As was discussed in section 3, central California is probably underlain by the stalled Monterey microplate (Figure 2) [Nicholson et al., 1994], and therefore a slab gap never existed in central California [Atwater and Stock, 1998]. We argue here that shear heating is also not required to explain the elevated heat flow of the Coast Ranges there. The higher heat flow is simply the consequence of reequilibration of the geothermal gradient following the cessation of subduction of the Monterey microplate. This microplate rotated clockwise, and subduction rate slowed, similar to the more recent history of the JdF plate. Subduction finally stopped at Chron 5E (18 Ma) as the northern end of the mid-oceanic ridge was subducted [Nicholson et al., 1994]. The stalled Monterey slab underlying the Coast Ranges was probably less than 4 Myr old, assuming a convergence rate of $30\text{--}40 \text{ km Myr}^{-1}$. We can use the thermal model of Figures 6a and 7 to calculate the heat flow as a function of time after the cessation of subduction. As discussed in section 5, the forearc region of the subduction zone is relatively cold during subduction even when it is underlain by a young oceanic lithosphere. However, when subduction stops, thermal reequilibration between the forearc and the underlying hot slab begins and the temperature gradient of the forearc rises. The predicted heat flows for a 2 and 4 Myr old subducted slabs 18 Myr after subduction ceased are 75 and 81 mW m^{-2} , respectively. Mean heat flow of 39 measurements in the central Coast Ranges is $83 \pm 3 \text{ mW m}^{-2}$, and the mean heat

flow of 17 newer measurements in boreholes in the Parkfield-Cholame area is $74 \pm 4 \text{ mW m}^{-2}$ [Sass et al., 1997]. We therefore argue that the heat flow regime in central California cannot be used to argue for or against viscous shear heating in the upper mantle. It is simply the consequence of its geological history as a subduction plate boundary.

9. Conclusions

We propose a "slab stretch model" to explain the interaction of plates at depth near the triple junction. In this model the geometrical gap formed owing to the northward migration of the triple junction is filled by stretched and thinned subducted Juan de Fuca plate. The stretching is in response to boundary forces acting on the plate, in particular, the northward push across the Mendocino Fracture Zone, and the southward (trench-parallel) component of subduction resistance. The thinning, estimated from simple geometrical considerations to be, on average, 27-37%, results in an elevated geothermal gradient. Locally, however, the amount of thinning may vary, resulting in higher or lower extension rates. The elevated geothermal gradient is equivalent to a 4 Ma oceanic lithosphere, still much cooler than that inferred by the slab gap model. In this thermal regime the composition and small volumes of Coast Ranges Neogene volcanic rocks are thought to be mainly due to dehydration melting of the fossil subducted oceanic crust. This model is consistent with heat flow measurements, thermobarometry, normal, shallow upper mantle velocities from tomographic inversion of earthquake travel times, and the existence of bright reflections in the high-velocity layer at the base of the crust. To study the effect of asthenospheric upwelling to shallow levels beneath the crust, we draw attention to the Inner Continental Borderland in southern California, which underwent local extension, possibly in a core complex mode, 18-20 Myr ago. The opening in the former forearc of the subduction zone probably extended to the fossil subducted plate, creating a slab gap. High heat flow, voluminous volcanism, a rather primitive isotopic composition of the magmas, and the absence of a high P wave velocity basal layer are observed in the Inner Continental Borderland in contrast to northern California. We also argue that the broad zone of high heat flow in central California, averaging 30 mW m^{-2} higher than that typical for continental regions, is neither due to a slab gap nor due to viscous shear heating in the upper mantle, as was previously suggested. It is simply the consequence of cessation of subduction of the Monterey microplate and the thermal reequilibration of the stalled microplate with the overlying Coast Ranges.

Acknowledgments. We thank Harley Benz for permission to publish Plate 2, Craig Nicholson and Stan Hart for illuminating discussions, Dave Scholl for his encouragement, David Okaya for use of his computer code, Chris Anton and Jeff Zwinakis for drafting several figures, and Peter Kelemen and Tom Brocher for reviewing earlier versions of this manuscript. Reviews by Nikky Godfrey, John Hole, and Craig Nicholson greatly improved the manuscript.

References

- Atwater, T., Plate tectonic history of the northeast Pacific and western North America, in *The Eastern Pacific Ocean and Hawaii*, edited by E. L. Winterer, D. M. Hussong, and R. W. Decker, pp. 29-72, Geol. Soc. Am., Boulder, Colo., 1989.

- Atwater, T., and J. Stock, Pacific-North America plate tectonics of the Neogene southwestern United States: An update, *Int. Geol. Rev.*, **40**, 375-402, 1998.
- Beaudoin, B.C., et al., Transition from slab to slabless: Results from the 1993 Mendocino triple junction seismic experiment, *Geology*, **24**, 195-199, 1996.
- Beaudoin, B.C., J.A. Hole, S.L. Klemperer, and A.M. Trehu, Location of the southern edge of the Gorda slab and evidence for an adjacent asthenospheric window: Results from seismic profiling and gravity, *J. Geophys. Res.*, **103**, 30,101-30,115, 1998.
- Benz, H.M., G. Zandt, and D.H. Oppenheimer, Lithospheric structure of northern California from teleseismic images of the upper mantle, *J. Geophys. Res.*, **97**, 4791-4807, 1992.
- Benz, H.M., B. Chouet, P.B. Dawson, J.C. Lahr, R.A. Page, and J.A. Hole, Three-dimensional *P* and *S* wave velocity structure of Redoubt volcano, *J. Geophys. Res.*, **101**, 8118-8128, 1996.
- Bohannon, R.G., and T. Parsons, Tectonic implications of post-30 Ma Pacific and North American relative plate motion, *Geol. Soc. Am. Bull.*, **107**, 937-959, 1995.
- Brace, W.F., and D.L. Kohlstedt, Limits on lithospheric stress imposed by laboratory experiments, *J. Geophys. Res.*, **85**, 6248-6252, 1980.
- Brocher, T.M., U.S. ten Brink, and T. Abramovitz, Synthesis of crustal seismic structure argues against a slab gap beneath coastal California, *Int. Geol. Rev.*, **41**, 263-274, 1999.
- Cole, R.B., and A.R. Basu, Nd-Sr isotopic geochemistry and tectonics of ridge subduction and middle Cenozoic volcanism in western California, *Geol. Soc. Am. Bull.*, **107**, 167-179, 1995.
- Crouch, J.K., and J. Suppe, Late Cenozoic tectonic evolution of the Los Angeles Basin and Inner California Borderland: A model for core complex-like crustal extension, *Geol. Soc. Am. Bull.*, **105**, 1415-1434, 1993.
- Defant, M.J., and M.S. Drummond, Subducted lithosphere-derived andesitic and dacitic rocks in young volcanic arc setting, *Nature*, **347**, 662-665, 1990.
- Dickinson, W.R., Tectonic implications of Cenozoic volcanism in coastal California, *Geol. Soc. Am. Bull.*, **109**, 936-954, 1997.
- Dickinson, W.R., and W.S. Snyder, Geometry of subducted plates related to San Andreas Transform, *J. Geol.*, **87**, 609-627, 1979a.
- Dickinson, W.R., and W.S. Snyder, Geometry of triple junctions related to San Andreas Transform, *J. Geophys. Res.*, **84**, 561-572, 1979.
- Dumitru, T.A., Effects of subduction parameters on geothermal gradients in forearcs, with an application to Franciscan subduction in California, *J. Geophys. Res.*, **96**, 621-641, 1991.
- Furlong, K.P., W.D. Hugo, and G. Zandt, Geometry and evolution of the San Andreas fault zone in northern California, *J. Geophys. Res.*, **94**, 3100-3110, 1989.
- Godfrey, N.J., and S.L. Klemperer, Ophiolitic basement to a forearc basin and implications for continental growth: The Coast Range/Great Valley ophiolite, California, *Tectonics*, **17**, 558-570, 1998.
- Godfrey, N., B.C. Beaudoin, S.L. Klemperer, and the Mendocino Working Group, Ophiolitic basement to the Great Valley forearc basin, California, from seismic and gravity data: Implications for crustal growth of the North American continental margin, *Geol. Soc. Am. Bull.*, **109**, 1536-1562, 1997.
- Hearn, B.C., J.M. Donnelly-Nolan, and F.E. Goff, The Clear Lake Volcanics: Tectonic setting and magma sources, *U.S. Geol. Surv. Prof. Pap.*, **1141**, 25-45, 1981.
- Heasler, H.P., and R.C. Surdam, Thermal evolution of coastal California with application to hydrocarbon maturation, *AAPG Bull.*, **69**, 1386-1400, 1985.
- Henstock, T.J., A. Levander, and J.A. Hole, Deformation in the lower crust of the San Andreas fault system in northern California, *Science*, **278**, 650-653, 1997.
- Hofmann, A.W., Chemical differentiation of the Earth: The relationship between mantle, continental crust, and oceanic crust, *Earth Planet. Sci. Lett.*, **90**, 297-314, 1988.
- Hole, J.A., B.C. Beaudoin, and T.J. Henstock, Wide-angle seismic constraints on the evolution of the deep San Andreas plate boundary by Mendocino triple junction migration, *Tectonics*, **17**, 802-818, 1998.
- Howie, J.M., K.C. Miller, and W.U. Savage, Integrated crustal structure across the south central California margin: Santa Lucia Escarpment to the San Andreas Fault, *J. Geophys. Res.*, **98**, 8173-8196, 1993.
- James, T.S., L.S. Hollister, and W.J. Morgan, Thermal modeling of the Chugach metamorphic complex, *J. Geophys. Res.*, **94**, 4411-4423, 1989.
- Johnson, C.M., and J.R. O'Neil, Triple junction magmatism: A geochemical study of Neogene volcanic rocks in western California, *Earth Planet. Sci. Lett.*, **71**, 241-262, 1984.
- Jove, C.F., and R.G. Coleman, Extension and mantle upwelling within the San Andreas fault zone, San Francisco Bay area, California, *Tectonics*, **17**, 883-890, 1998.
- Kelsey, H.M., and G.A. Carver, Late Neogene and Quaternary tectonics associated with northward growth of the San Andreas transform fault, northern California, *J. Geophys. Res.*, **93**, 4797-4819, 1988.
- Lachenbruch, A.H., and J.H. Sass, Thermomechanical aspects of the San Andreas fault system, in *Tectonic Problems of the San Andreas Fault System*, edited by R.L. Kovach, and A. Nur, pp. 192-205, Stanford University Press, Stanford, Calif., 1973.
- Lachenbruch, A.H. and J.H. Sass, Heat flow and energetics of the San Andreas fault zone, *J. Geophys. Res.*, **85**, 6977-6989, 1980.
- Lee, T.-C., and T.L. Henyey, Heat flow through the southern California Borderland, *J. Geophys. Res.*, **80**, 3733-3743, 1975.
- Levander, A., T.J. Henstock, A.S. Meltzer, B.C. Beaudoin, A.M. Trehu, and S.L. Klemperer, Fluids in the lower crust following Mendocino triple junction migration: Active basaltic intrusion?, *Geology*, **26**, 171-174, 1998.
- Liu, M., and K.P. Furlong, Cenozoic volcanism in the California Coast Ranges: Numerical solutions, *J. Geophys. Res.*, **97**, 4941-4951, 1992.
- McKenzie, D., and M.J. Bickle, The volume and composition of melt generated by extension of the lithosphere, *J. Petrol.*, **29**, 625-679, 1988.
- McLaughlin, R.J., W.V. Sliter, D.H. Sorg, P.C. Russel, and A.M. Sarna-Wojcicki, Large-scale right-slip displacement on the East San Francisco Bay Region fault system, California: Implications for location of late Miocene to Pliocene Pacific plate boundary, *Tectonics*, **15**, 1-18, 1996.
- Miller, K.C., J.M. Howie, and S.D. Ruppert, Shortening within underplated oceanic crust beneath the central California margin, *J. Geophys. Res.*, **97**, 19,961-19,980, 1992.
- Molnar, P., Brace-Goetze Strength profiles, the partitioning of strike-slip and thrust faulting at zones of oblique convergence, and the stress-heat flow paradox of the San Andreas fault, in *Fault Mechanics and Transport Properties of Rocks*, edited by T.F. Wong and B. Evans, pp. 435-459, Academic, San Diego, Calif., 1992.
- Nichols, G.T., P.J. Wyllie, and C.R. Stern, Experimental melting of pelagic sediment, constraints relevant to subduction, in *Subduction: Top to Bottom*, *Geophys. Monog. Ser.*, vol. 96, edited by G. E. Bebout et al., pp. 293-298, AGU, Washington, D.C., 1996.
- Nicholson, C., C.C. Sorlien, T. Atwater, J.C. Crowell, and B.P. Luyendyk, Microplate capture, rotation of the western Transverse Ranges, and initiation of the San Andreas transform as a low-angle fault system, *Geology*, **22**, 491-495, 1994.
- Oppenheimer, D., et al., The Cape Mendocino, California, earthquakes of April 1992: Subduction at the triple junction, *Science*, **261**, 433-438, 1993.
- Page, B.M., and T.M. Brocher, Thrusting of the central California margin over the edge of the Pacific plate during the transform regime, *Geology*, **21**, 635-638, 1993.
- Parsons, T., and P.E. Hart, Dipping San Andreas and Hayward faults revealed beneath San Francisco Bay, California, *Geology*, **27**, 839-842, 1999.
- Peacock, S., Thermal and petrologic structure of subduction zones, in *Subduction: Top to Bottom*, *Geophys. Monog. Ser.*, vol. 96, edited by G. E. Bebout et al., pp. 119-133, AGU, Washington, D.C., 1996.
- Prescott, W.H., and S.-B. Yu, Geodetic measurement of horizontal deformation in the northern San Francisco Bay region, California, *J. Geophys. Res.*, **91**, 7475-7484, 1986.
- Sass, J.H., C.F. Williams, A.H. Lachenbruch, S.P. Galanis, and F.V. Grubb, Thermal regime of the San Andreas fault near Parkfield, California, *J. Geophys. Res.*, **102**, 27575-27,585, 1997.
- ten Brink, U.S., J. Zhang, T.M. Brocher, D.A. Okaya, K.D., Klitgord, and G.S. Fuis, Geophysical evidence for the evolution of the California Inner Continental Borderland as a metamorphic core complex, *J. Geophys. Res.*, in press, 1999.
- van der Beukel, J., and R. Wortel, Thermomechanical modelling of arc-trench regions, *Tectonophysics*, **154**, 177-193, 1988.
- Vedder, J.G., Regional geology and petroleum potential of the southern California Borderland, in *Geology and Resource Potential of the Continental Margin of Western North America and Adjacent Ocean Basins: Beaufort Sea to Baja California*, edited by D. W. Scholl, A. Grantz and J. G. Vedder, pp. 403-447, Circum-Pac. Council for Energy and Miner. Resour., Houston, TX, 1987.
- Walcott, D., Neogene tectonics and kinematics of western North America, *Tectonics*, **12**, 326-333, 1993.
- Wang, K., J. He, and E.E. Davis, Transform push, oblique subduction resistance, and intraplate stress of the Juan de Fuca plate, *J. Geophys. Res.*, **102**, 661-674, 1997.
- Wilson, D.S., A kinematic model for the Gorda deformation zone as a diffuse southern boundary of the Juan de Fuca plate, *J. Geophys. Res.*, **91**, 10,259-10,269, 1986.
- Wyllie, P.J., and M.B. Wolf, Amphibolite dehydration-melting: Sorting out the solidus, in *Magmatic Processes and Plate Tectonics*, edited by H. M. Prichard et al., pp. 405-416, Geol. Soc. of London, London, 1993.
- Zandt, G., and K.P. Furlong, Evolution and thickness of the lithosphere beneath coastal California, *Geology*, **10**, 376-381, 1982.

P.C. Molzer and U.S. ten Brink, U.S. Geological Survey, 384 Woods Hole Rd., Woods Hole, MA 02543.
(utenbrink@nobska.er.usgs.gov)
N. Shimizu, Woods Hole Oceanographic Institution, Woods Hole, MA 02543.

(Received February 10, 1999;
revised June 30, 1999;
accepted July 27, 1999.)